STUDY OF BEAM DYNAMICS DURING THE CROSSING OF THE THIRD-ORDER RESONANCE AT VEPP-4M

S. Glukhov, E. Levichev, O. Meshkov, S. Nikitin, I. Nikolaev, P. Piminov, A. Zhuravlev,
BINP, Novosibirsk, Russia

Abstract

The influence of resonances on beam dynamics in storage rings is of a substantial interest to accelerator physics. For example, a fast crossing of resonances occurring in the damping rings of future linear colliders during the beam damping (due to the incoherent shift) can result in a loss of particles. We have studied experimentally the crossing of resonance near the working point of the VEPP-4M storage ring. Observation of the beam sizes and particle losses was performed with a single-turn time resolution. Comparison with the numerical simulation has been made and will be presented alongside the experimental results.

INTRODUCTION

A series of experimental studies of the beam passage through the third-order betatron resonance was performed at the VEPP-4M electron storage ring in Novosibirsk during the last two years [1]. This paper summarizes the recent results obtained in these experiments.

The interest to this experimental work was inspired by the involvement of BINP in the carbon ion therapy project [2], where the resonance extraction of the ion beam is foreseen, and by the study of beam dynamics with strong damping and space charge in the CLIC damping ring [3].

It is essentially important for the ion beam extracted at the resonance with therapeutic purpose to have highly predictable, controllable and constant extraction rate. Meanwhile, this rate is very sensitive to the extraction conditions, PS ripple, aperture limitation, etc. This fact calls forth an importance of the experimental measurements of the beam behavior during the resonance crossing.

The beam damped in the damping ring with the emittance reduced by 2-3 orders of magnitude. A strong space charge potential together with highly nonlinear lattice causes the core beam tune shift (mainly in the vertical direction) as much as ~0.1-0.2, while the particles in the beam tail are smeared in the betatron tunes due to the tune-amplitude dependence. During the damping, the particles cross many resonances and, as a computer simulation has shown, may be either trapped inside the stable resonance islands or lost at the unstable resonances. This mechanism may influence the quality of the beam extracted from the damping ring to the linear collider.

In this report we discuss the results of experimental study of the resonance passage at the VEPP-4M collider. The third-order resonance $3\nu_z = 23$ was traversed by the electron beam with the variable speed. During the experiment the resonance strength could be changed by a single skew-sextupole magnet while the nonlinear detuning was controlled by a number of the octupole lenses. Different parameters such as particles loss rate, beam size and transverse distribution, space phase trajectories, amplitude dependent tune shift, etc. were measured.

MEASUREMENT SETUP

The VEPP-4M electron-positron collider with the maximum energy of 5.5 GeV is operating now at ~1.8 GeV in the region of the ψ-meson family. The collider is equipped with a number of beam diagnostics, which allow the measurement of different parameters and the study of nonlinear motion. The phase space trajectories are registered by the excitation of the coherent beam motion with the help of the fast electromagnet kicker with 50 ns 30 kV pulse. To measure the beam centroid motion, BPMs in the turn-by turn mode are used. The BPM resolution is ~50 μm.

Particles loss and the beam distribution tails are measured by a set of scintillator counters inserted into the vacuum chamber. The counter can be moved by a step-motor in and out of the beam with the accuracy better than 0.1 mm. All measurements were performed at the low electron current of ~0.5 mA to avoid coherent effects. The chromaticity was set to ~+0.5÷+1 for both planes unless the synchrobetatron resonances are observed. We changed the vetical betatron tune by varying the quadrupole current. The minimal rate provided by the quadrupole power supply is $\Delta\nu_z = 0.01$ at 40 ms.

To measure a single-turn transverse beam distribution during tens of thousands of turns we have developed a unique device [4] based on the multi-anode photomultiplier R5900U-00-L16 HAMAMATSU. This device is capable of recording a transversal profile of a beam at 16 points at one turn during 2^{17} turns of a beam.

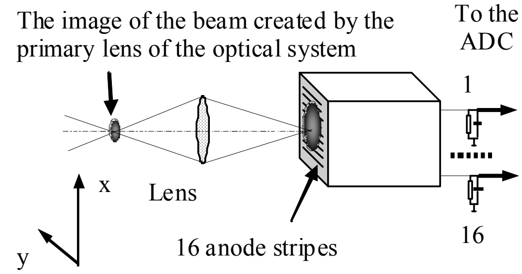

Figure 1: Optical layout of the diagnostics. The lens sets up a beam image on the photocathode of the MAPMT. The radial profile measurement is shown.

The optical arrangement (Fig.1) allows us to change the beam image magnification on the cathode of MAPMT from 6× to 20×, which is determined by the experimental demands. The set of remote controlled grey filters, included into optical diagnostics, allows selecting a suitable level of the light intensity with the dynamic range of about 10^3.

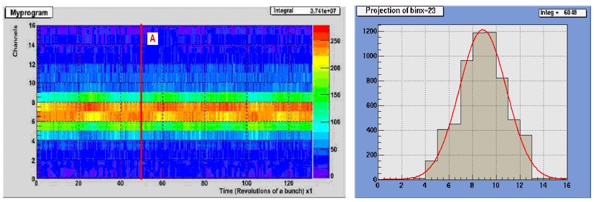

Figure 2: The vertical beam profile vs. revolution number (left plot). Colors indicate the beam intensity. Single shot vertical beam profile fitted by the Gauss function (right plot).

The example of the vertical beam profile measurement as a function of the turn number during the resonance crossing with the maximum speed and the nonlinear detuning close to zero is shown in Fig.2, left. A cross-section of the plot along the line *A* is depicted in Fig.2, right.

NONLINEAR DETUNING

As it is known, the phase space topology of the third-order resonance depends on the nonlinearity, which in the second order of approximation has the form

$$\Delta\nu_x = C_{xx}A_x^2 + C_{xz}A_z^2 \quad \text{and} \quad \Delta\nu_z = C_{zx}A_x^2 + C_{zz}A_z^2 .$$

In VEPP-4M two families of the octupole magnets SEOQ and NEOQ with the maximum current ±25 A, placed symmetrically to the IP at the azimuth with $\beta_z >> \beta_x$, can control the tune-amplitude dependence coefficients.

The experimental results of the vertical tune measurement as a function of the vertical kick amplitude for different polarity of the octupole current are depicted in Fig.3

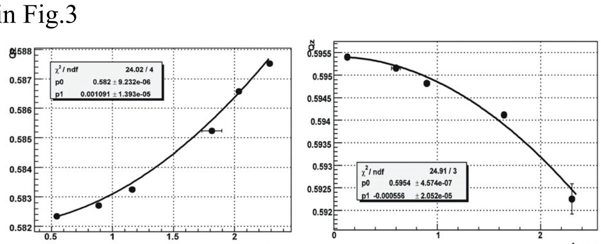

Figure 3: Vertical tune vs. amplitude for different currents in the octupoles. Polarity changing gives the tune shift term change from $C_{zz} = 1\times10^{-3}$ mm^{-2} to $C_{zz} = -0.5\times10^{-3}$ mm^{-2}.

The values of the tune-amplitude dependence terms as a function of the octupole current are listed in Table 1.

Table 1: Tune-amplitude dependence coefficients (*O* is the octupoles current)

$10^4 \cdot C_{nm}$ (mm^2)	*O = 0 A*	*–25 A*	*+25 A*
C_{xx}	1.6	4.4	–0.4
C_{xz}	0	–6.6	2.2
C_{zx}	0	–11.6	6.6
C_{zz}	0	11	–5.6

With the octupoles switched off, the vertical nonlinear term C_{zz} is equal to zero, the resonance trajectories outside the central area are unbound (Fig.10) and for the exact resonance condition the motion of all the particles is unstable. One can expect that the passing of such resonance causes beam intensity loss with the rate depending on the passing speed. Below, we refer this case as the crossing with low nonlinear detuning.

On the contrary, for –25 A excitation current, the term C_{zz} is maximal and three stable islands appear outside the central resonance region (Fig.4). This case corresponds (depending on the crossing rate) to the particles trapping inside the islands and to the transporting outward the beam axis. This case is referred below as the resonance crossing with high nonlinear detuning.

RESONANCE DRIVING TERM

Several approaches were applied to determine the resonance driving term. A turn-by-turn measurement of the phase space trajectories for different kick amplitude (Fig.11) allows the estimation of the resonance driving term from the following considerations. For the resonance $3\nu_z = n$, a perturbated term of the Hamiltonian

$$H_1 = (2J_z)^{3/2}\sum_n A_{3n}\cos(3\varphi_z - n\theta),$$

where A_{3n} are the relevant Fourier harmonics of the sextupole perturbation, allows us to obtain the second-order invariant

$$\bar{J}_z \approx J_z + a_{3n}J_z^{3/2}\cos 3\varphi_z \approx const, \quad a_{3n} = 3\sqrt{8}\,\frac{A_{3n}}{3\nu_z - n},$$

which gives the following estimation of the main perturbation harmonic from the measured curve $J_z(\varphi_z)$

$$a_{3n} \approx \frac{J_{\max} - J_{\min}}{J_{\max}^{3/2} + J_{\min}^{3/2}}.$$

In our case the estimation of the resonance driving term from the experimental data gives the value of $A_{3,2}$ = 0.03÷0.07 mm$^{-1/2}$ depending on the operation mode and lattice tuning. Other approaches, such as the dynamic aperture measurement either from the beam life time in the vicinity of the resonance or as the maximum kick amplitude, give consistent values of the main resonance harmonic amplitude.

RESONANCE CROSSING WITH HIGH NONLINEAR DETUNING

A standard isolated resonance Hamiltonian in the action-angle variable has the following form

$$H = \delta(\theta)\cdot I + \alpha_0 \cdot I^2 + A_n \cdot I^{n/2} \cos m\varphi, \qquad (1)$$

with the nonlinear tune shift coefficient $\alpha_0 = C_{zz}/\beta_z$, the driving term strength A_n and the distance from the resonance $\delta(\theta)$ that varies with time θ. A sketch of the phase space portrait corresponding to the Hamiltonian (1) is plotted in Fig.4.

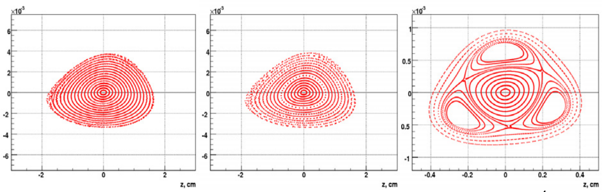

-2.66×10^{-3} $\delta(\theta) = 0$ 3.4×10^{-4}

Figure 4: Phase trajectories evolution during the stable resonance crossing.

For relevant tune-amplitude dependence, three stable resonance islands are created at the phase space plot when the betatron tune crosses the resonance value (Fig.4). The sign of nonlinearity should correlate with the tune variation direction: for the positive nonlinearity the tune should be decreased to generate the islands at the exact resonant value.

The turn-by-turn measurement also allows obtaining similar trajectories (Fig.5).

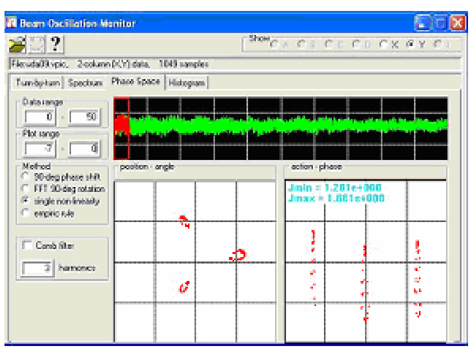

Figure 5: Measured trajectories inside the resonance island.

An adiabatic condition of the particles capturing into the resonance island in the case of the third-order resonance has the form [5]

$$I_a > \left(\frac{\nu'}{6\cdot\alpha_0\cdot A_3} \right)^{1/3},$$

where $\nu' = d\nu/d\theta$ is the resonance crossing rate and I_a is the captured particle amplitude. According to this criterion, the fraction of the trapped particles grows with the increasing of the nonlinear detuning α_0 and the decreasing of the crossing rate. Estimation for VEPP-4M shows that for the maximum nonlinearity (the octupole current is –25 A) and the resonant term A_3 ~ 0.05 mm$^{-1/2}$, the resonance crossing rate to trap noticeable fraction of the particles should be in the range of 0.1-1 s.

The evolution of the vertical beam profile during the crossing of the resonance $3\nu_z = 23$ with high nonlinearity is shown in Figs.6-8. In Fig.8 the island formation and the particles capture and transportation to the high amplitudes are clearly seen.

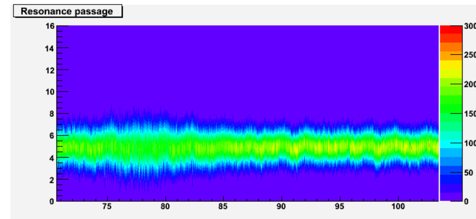

Figure 6: Tune range is Q_z = 0.6608÷0.6717; crossing time is 40 ms. For high rate neither beam size change nor particles capture is seen.

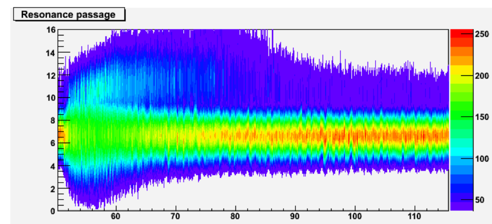

Figure 7: The same as in Fig.5 but the crossing time is 0.3 s. A beam blow-up and some evidence of the particles trapping are observed.

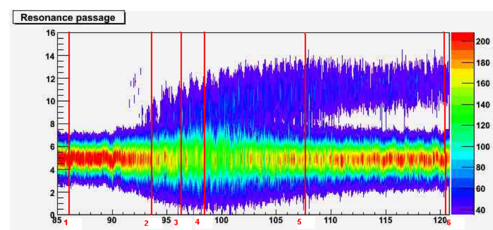

Figure 8: Time evolution of the vertical beam profile in the case of the particle trapping in the resonance island ($\Delta t = 3$ s).

Transverse cross-sections of the evolution plot in Fig.8 in different moments of the resonance passage are given in Fig.9.

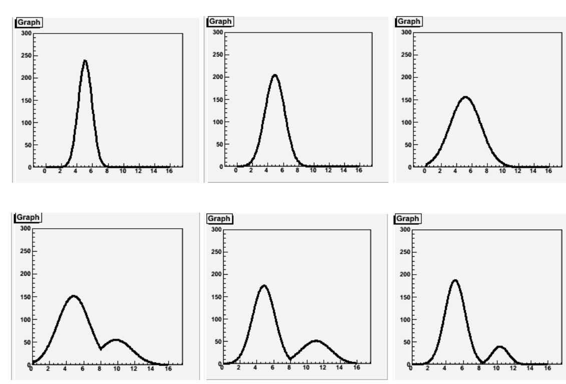

Figure 9: Transverse distribution of the beam profile (Gauss fit of the MAPMT 16 channels) corresponding to the different moments indicated by the red lines in Fig.8.

RESONANCE CROSSING WITH LOW NONLINEAR DETUNING

If in Hamiltonian (1) one takes $\alpha_0 = C_{zz} = 0$, the island structure does not appear during the resonance crossing. The phase trajectories corresponding to this case are shown in Fig.10 (computer simulation) and Fig.11 (turn-by-turn observation).

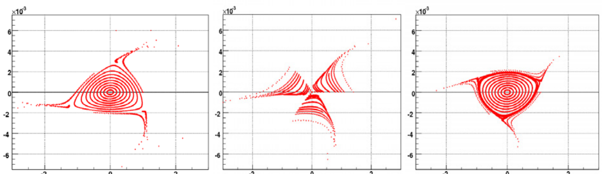

-2.66×10^{-3} $\delta(\theta)=0$ 3.34×10^{-3}

Figure 10: Phase space portrait for the crossing of the unstable third-order resonance.

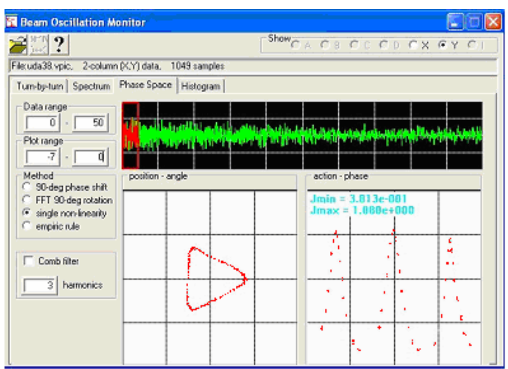

Figure 11: Measured phase trajectories close to the third-order resonance.

As there are no stable trajectories exactly on the resonance, one can expect loss of the beam intensity instead of the particles trapping in the islands. The value and the rate of the loss depend of the resonance passing speed. If the speed is high enough, not all the particles from the beam are lost; some of them can be captured back to the central resonance area.

The adiabatic criterion in this case can be formulated as follows. All the particles will be lost from the beam during the unstable resonance crossing if the crossing rate $\nu' = d\nu / d\theta$ satisfies the relation [6]

$$\nu' << A_3^2 \cdot \varepsilon_z / 8\pi ,$$

where ε_z is the beam emittance.

A typical particles loss profile during the unstable resonance crossing is shown in Fig.12. One can see that the signal of the loss rate measured by the vertical scintillator probe in the vacuum chamber has highly irregular spiky profile, which can be explained by the ripple and instabilities of the magnet power supplies.

The theory in [6] allows defining the particles loss rate curve. The analytic expressions were applied to the measurement results and the comparison is presented in Fig.13 and Fig.14. One can see that the theory predicts the sharp edge of the loss rate curve depending on the resonance crossing direction (with the tune increase or decrease).

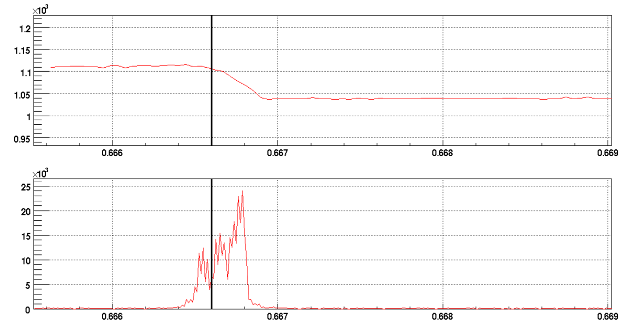

Figure 12: Total intensity decrease (upper plot) and particles loss rate (lower plot) during the resonance crossing. Tune change 0.6687→0.6653 for 1 s, I = 0.212 → 0.214

And, indeed, the same behaviour is observed in the experimental results in Fig.13-14. However, despite the relative loss rate profiles found theoretically and experimentally are rather consistent, the absolute value of the intensity loss is differs much.

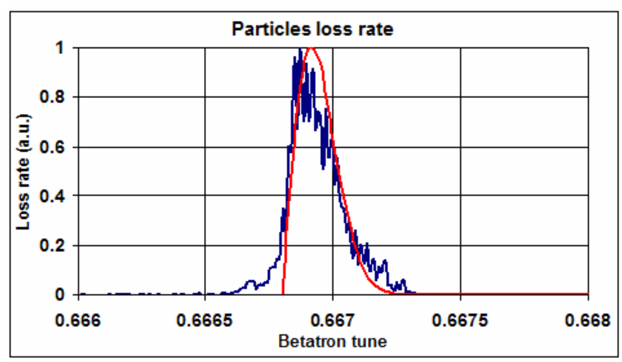

Figure 13: The vertical betatron tune change $\Delta\nu_z$ = 0.6653→ 0.6685 for 1 s, I = 0.183→0.181

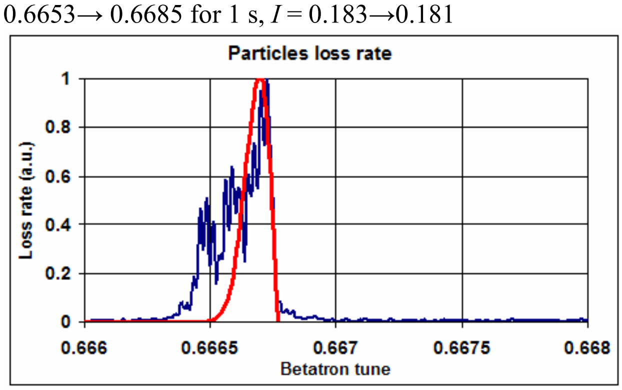

Figure 14: Tune shift if 0.6687→0.6653 for 1 s, I = 0.212→0.214

Now we are trying to explain it either by the radiation damping or the residue nonlinearity.

SYNCHROBETATRON RESONANCES OBSERVATION

All previous measurements were performed with the chromaticity compensated to +0.5…+1. The following studies concern the VEPP-4M lattice with a rather high vertical chromaticity that was controlled by the sextupole magnets. The particles loss was observed to explore the influence of the synchrobetatron satellites.

In Fig.15 the particles loss rate with the vertical chromaticity increased to 9.5 is shown. The distance between the main resonance and the satellites just corresponds to the synchrotron tune of 0.005. All the beam intensity was lost during the passing of the third-order resonance with two satellites.

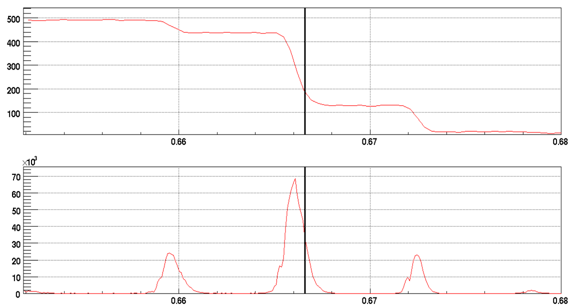

Figure 15: $\Delta\nu_z = 0.02$ for 10 s, $I = 0.120 \rightarrow 0$, $\xi_x = 0.5$, $\xi_z = 9.5$

Further increasing of the vertical chromaticity generates growing of the synchrobetatron satellites number. In Fig.16 one can see two satellites around the main resonance line.

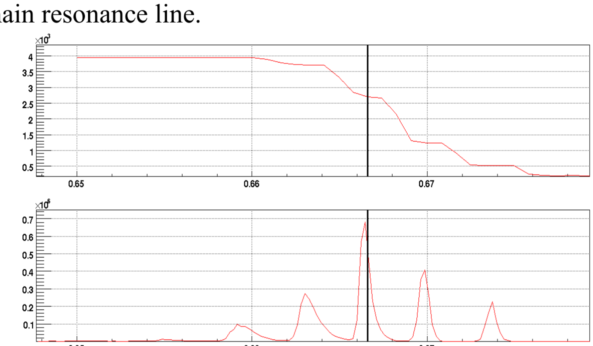

Figure 16: The same as for Fig.15 but with the vertical chromaticity increased to 15.5.

CONCLUSIONS

The beam dynamics during the vertical betatron third-order resonance was studied experimentally. Two specific cases were separately explored.

The first case relates to the rather high value of the vertical tune-amplitude dependence. It was shown that with the adiabatic crossing rate, the resonance islands can capture some fraction of particles and transport them to the high amplitudes. The trapping capability can be controlled by the octupole magnets. This fact can be useful to provide high performance of the damping rings: the nonlinear detuning coefficients should be adjusted during the damping to prevent particles captures in the nonlinear resonances.

Another case relates to the low value of the amplitude-dependent tune shift. In this case no resonance islands appear and significant portion of the beam intensity can be lost during the resonance passage. This case is sensitive to the beam damping and the residue nonlinearity as well as to the ripple of the power supply system.

Additionally, the crossing of the synchrobetatron resonances was studied experimentally. It was shown that the particles loss increased at the satellite resonances.

REFERENCES

[1] V.Kiselev et al. Proc. of EPAC08, Genoa, Italy, TUOBG02 (2008) 965-967.

[2] E.B.Levichev et al., Proc. of RUPAC06, Novosibirsk, Russia (2006) 363-365.

[3] E.Levichev, P.Piminov and D.Shatilov, submitted to PRST (2009).

[4] O.I.Meshkov et al. VEPP-4M optical beam profile monitor with one-turn temporal resolution, Proc.of EPAC’04, Lucerne (2004) 2733-2735.

[5] A.Chao and M.Month, Particle trapping during passage through a high-order nonlinear resonance, NIM 121 (1974) 129-138.

[6] S.Nikitin, Proc. of EPAC06, Edinburgh, Scotland, WEPCH086 (2006) 2119-2121.